

## Limiting the relative orientation of bridged cyclopentadienyl anions. Mono- and dianions derived from 4,4,8,8-tetramethyltetrahydro-4,8-disila-s-indacenes

Johann. Hiermeier, Frank H. Koehler, and Gerhard. Mueller

*Organometallics*, 1991, 10 (6), 1787-1793 • DOI: 10.1021/om00052a026 • Publication Date (Web): 01 May 2002

Downloaded from <http://pubs.acs.org> on March 8, 2009

### More About This Article

---

The permalink <http://dx.doi.org/10.1021/om00052a026> provides access to:

- Links to articles and content related to this article
- Copyright permission to reproduce figures and/or text from this article



ACS Publications  
High quality. High impact.

# Limiting the Relative Orientation of Bridged Cyclopentadienyl Anions. Mono- and Dianions Derived from 4,4,8,8-Tetramethyltetrahydro-4,8-disila-s-indacenes

Johann Hiermeier, Frank H. Köhler,\* and Gerhard Müller†

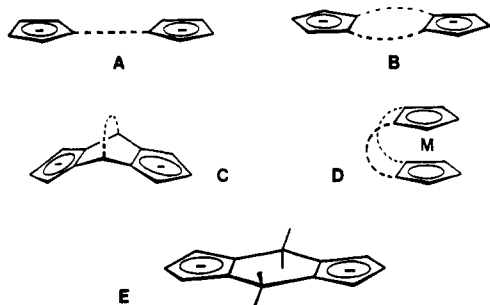
Anorganisch-chemisches Institut, Technische Universität München, D-8046 Garching, FRG

Received November 1, 1990

Two isomers of 4,4,8,8-tetramethyltetrahydro-4,8-disila-s-indacene have been deprotonated under various conditions to give novel anions in which a cyclopentadienyl (Cp) and a cyclopentadiene or two Cp's are doubly bridged by  $\text{Me}_2\text{Si}$  fragments to give the monoanion **3** or the dianion **4**. Use of NaH or 1 equiv of *n*-BuLi selectively yielded **3** whereas KH or 2 equiv of *n*-BuLi gave **4**. Temperature-dependent NMR spectroscopy showed the two enantiomers **3a/b** of the monoanion to undergo both a degenerate and a nondegenerate silatropic rearrangement with a barrier of  $E_a = 48.5 \text{ kJ mol}^{-1}$ . The intermediate in this process contains a 1,3-disilacyclopent-4-ene fragment which is energetically unfavorable so that its abundance is only 2.4% at 29 °C. The dilithium derivative  $4\text{Li}_2$  of the dianion forms predominantly solvent-separated or contact ion pairs in solution depending on the solvent. The solid-state structure of  $4\text{Li}_2(\text{TMEDA})_2$  was determined by X-ray structure analysis: triclinic,  $P\bar{1}$  (No. 2),  $a = 8.216(1) \text{ \AA}$ ,  $b = 9.014(1) \text{ \AA}$ ,  $c = 11.527(1) \text{ \AA}$ ,  $\alpha = 111.10(1)^\circ$ ,  $\beta = 100.66(1)^\circ$ ,  $\gamma = 88.85(1)^\circ$ ,  $R_w = 0.075$  for 154 refined parameters and 2193 observables. Anti orientation was found for the  $\text{Li}(\text{TMEDA})$  moieties, and a slight double folding, for the dianionic skeleton.

## Introduction

Among the various possibilities to bridge two cyclopentadienyl (Cp) ligands emphasis may be laid on the electronic and steric properties of the bridge. Both will influence the interaction between the metal fragments bound to the Cp's, and in many cases these factors will not be independent. From the steric point of view branching two Cp's by a single bond or a chain like in A will lead to



Key: (a)  $\text{Me}_2\text{SiCl}_2$ ; (b) *n*-BuLi.

we report on the formation and the properties of corresponding anions.

## Results and Discussion

The starting  $\text{Me}_2\text{Si}$ -bridged cyclopentadienes **2a/b** are known from the work of Sakurai,<sup>5</sup> Barton,<sup>6</sup> Ustynyuk,<sup>7</sup> and Jones.<sup>8</sup> The most convenient access is the three-step procedure summarized in Scheme I, which allowed us to routinely obtain 45-g quantities in an overall yield of about

a maximum of freedom with respect to their relative orientation. In these cases it will be difficult to predetermine the interaction in the corresponding dinuclear metal derivatives if no additional bridge is provided. A minimum of orientational freedom for the Cp-metal fragments can be achieved by a rigid unsaturated bridge<sup>1</sup> including type B,<sup>2</sup> which may be also looked upon as a simplification of the bicyclic bridge in C.<sup>3</sup>

When the chains in A and B are long enough, metallocenophanes are alternatives to bridged species. For instance, type B ligands are present in D, and corresponding ferrocenophanes with tetra- and trimethylene bridges are known.<sup>4</sup> Shortening the bridges will disfavor the metallocenophane structure leading to bent metallocenes as conceivable borderline cases, and with type E ligands bridging of two metal-containing fragments should again be possible. E attracted our attention because its flexibility should be intermediate between A and C or the fully conjugated version of B. We have therefore set out to explore the chemistry of the disila derivative of E. Here

(1) (a) Katz, T. J.; Śluzarek, W. *J. Am. Chem. Soc.* **1980**, *102*, 1058. (b) Katz, T. J.; Śluzarek, W. *J. Am. Chem. Soc.* **1979**, *101*, 4259. (c) Sudhakar, A.; Katz, T. J. *J. Am. Chem. Soc.* **1986**, *108*, 179. (d) Lynch, T. J.; Helvenston, M. C.; Rheingold, A. L.; Staley, D. L. *Organometallics* **1989**, *8*, 1959.

(2) (a) Katz, T. J.; Schulmann, J. *J. Am. Chem. Soc.* **1964**, *86*, 3169. (b) Katz, T. J.; Balogh, V.; Schulmann, J. *J. Am. Chem. Soc.* **1968**, *90*, 734. (c) Gitany, R.; Paul, I. C.; Acton, N.; Katz, T. J. *Tetrahedron Lett.* **1970**, 2733. (d) Ijima, S.; Motoyama, I.; Sano, H. *Chem. Lett.* **1979**, 1349. (e) Bell, W. L.; Curtis, C. J.; Eigenbrot, C. W., Jr.; Pierpont, C. G.; Robbins, J. L.; Smart, J. C. *Organometallics* **1987**, *6*, 266. (f) Bell, W. L.; Curtis, C. J.; Miedaner, A.; Eigenbrot, C. W., Jr.; Haltiwanger, R. C.; Pierpont, C. G.; Smart, J. C. *Organometallics* **1988**, *7*, 691.

(3) (a) Atzkern, H.; Köhler, F. H.; Müller, R. *Z. Naturforsch., B: Anorg. Chem. Org. Chem.* **1990**, *45*, 329. (b) Atzkern, H.; Huber, B.; Köhler, F. H.; Müller, G.; Müller, R. *Organometallics* **1991**, *10*, 238.

(4) (a) Hisatome, M.; Watanabe, N.; Sakamoto, T.; Yamakawa, K. *J. Organomet. Chem.* **1977**, *125*, 79. (b) Hillman, M.; Fujita, E.; Dauplaise, H.; Kwick, A.; Kerber, A. C. *Organometallics* **1984**, *3*, 1170 and references therein.

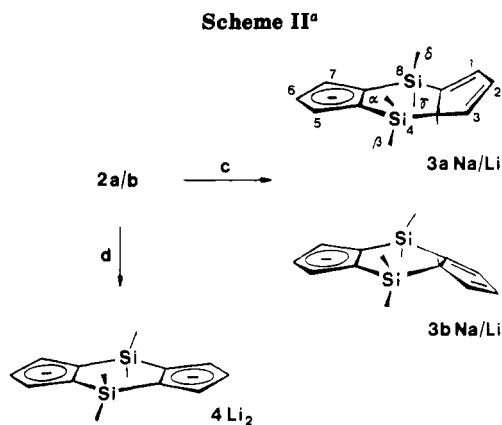
(5) Nakadaira, Y.; Sakaba, H.; Sakurai, H. *Chem. Lett.* **1980**, 1071.

(6) Barton, T. J.; Burns, G. T.; Arnold, E. V.; Clardy, J. *Tetrahedron Lett.* **1981**, *22*, 7.

(7) Zemlyanskii, N. N.; Borisova, I. V.; Luzikov, Yu. N.; Ustynyuk, Yu. A.; Kolosova, N. D.; Beletskaya, I. P. *J. Org. Chem. USSR (Engl. Transl.)* **1981**, *17*, 1174.

(8) Jones, P. R.; Rozell, Jr., J. M.; Campbell, B. M. *Organometallics* **1985**, *4*, 1321.

\* Present address: Fakultät für Chemie, Universität Konstanz, D-7750 Konstanz, FRG.



35%. When the procedure of Shologon et al.<sup>9</sup> was followed in step a, the yield of **1** was much lower than stated by these authors whereas in Schaaf's procedure<sup>10</sup> we found CpNa more advantageous than CpLi.

When the cheaper *n*-BuLi was used instead of *t*-BuLi in step b, the isolated yield of **2** was comparable to that found by GLC analysis.<sup>8</sup> Nucleophilic attack at silicon occurred as a side reaction. This became evident from the isolation of ferrocene substituted by a *n*-BuMe<sub>2</sub>Si group after further reaction of the cyclopentadienes with iron(II) chloride.<sup>11</sup>

Like other silylated cyclopentadienes, **2a/b** are susceptible to hydrolysis. Thus, a 2 M solution of **2a/b** in acetone containing 0.5% of water only showed the <sup>13</sup>C NMR signals of cyclopentadiene<sup>12</sup> after a few days and those of the dimer<sup>13</sup> after 2 weeks. It has been established by X-ray crystallography that **2a** is present in the solid state<sup>14</sup> whereas only incomplete <sup>1</sup>H and no <sup>13</sup>C data are available in the literature.<sup>5,6</sup> We have therefore recorded the <sup>29</sup>Si, <sup>13</sup>C, and <sup>1</sup>H NMR spectra at room temperature (see Experimental Section for details) and found the number of signals expected for the structures of **2a/b** shown in Scheme I. The protons of the Cp parts were identified by their characteristic<sup>15</sup>  $\delta$  and <sup>3</sup>J<sub>HH</sub> values, H2 and H3 of **2a/b** were distinguished by their <sup>4</sup>J<sub>HH</sub> values, and H $\alpha$  of **2a** or H $\beta$  or **2b** could be identified because a model showed that they are shielded by the neighboring double bonds. On this basis a suggestion was made for the assignment of H $\alpha$ / $\gamma$ / $\delta$  of **2b**. The <sup>13</sup>C signals were identified by selective decoupling experiments.

Owing to the fluxionality of **2a/b**, which has been already mentioned by Barton et al.,<sup>6</sup> severe broadening of the <sup>13</sup>C and <sup>1</sup>H resonances at elevated temperature and a striking simplification of the spectra were observed. Fourteen <sup>1</sup>H signals that were present at room temperature for the two isomers were averaged to give only three at 170 °C in biphenyl-*d*<sub>10</sub> with  $\delta$ (<sup>1</sup>H) 0.03, 5.22, and 6.61 for H $\alpha$ - $\delta$ , H1/3a/5/7a, and H2/3/6/7. At 170 °C the resonance at 5.22 ppm had a half-width of 250 Hz, which means that the high-temperature-limiting spectrum was not yet at-

**Table I.** <sup>13</sup>C and <sup>1</sup>H NMR Results for 4Li<sub>2</sub>

	position of nuclei <sup>a</sup>			CH <sub>3</sub>
	3a/8a, 4a/7a	1/3, 5/7	2/6	
$\delta$ ( <sup>13</sup> C) <sup>b</sup>	121.45	113.64	108.60	4.52
$\delta$ ( <sup>13</sup> C) <sup>c</sup>	119.70	111.62	108.05	5.17
<sup>1</sup> J(CH) <sup>c,f</sup>		152.6	151.9	114.4
$\delta$ ( <sup>1</sup> H) <sup>b</sup>		6.20	6.01	0.24
<sup>3</sup> J(HH) <sup>b,g</sup>		2.9 <sup>d</sup>	2.9 <sup>e</sup>	

<sup>a</sup>Numbering shown in Scheme II. <sup>b</sup>THF-*d*<sub>8</sub>/TMEDA (4/1). <sup>c</sup>HMPT. <sup>d</sup>Doublet. <sup>e</sup>Triplet. <sup>f</sup>J values in Hz.

tained. This problem was more serious in <sup>13</sup>C NMR spectroscopy where the 16 signals of **2a/b** should be reduced to 4. However, at 170 °C we could identify only three with  $\delta$ (<sup>13</sup>C) -4.6, 134.3, and 146.1 for C $\alpha$ - $\delta$ , C2/3/6/7, and C4a/8a; the signal of C1/3a/5/7a was still too broad to be detected. The mechanism underlying the fluxional behavior is similar to that of the monodeprotonated derivative, which is discussed below.

**Deprotonation of 2a/b.** Depending on the reaction conditions, only one or both acidic hydrogen atoms of **2a/b** could be removed. As shown in Scheme II, the reaction with sodium hydride sand gave the monoanion, which should be present as a mixture of enantiomers **3a/b** with sodium as counterion. The reaction was very slow and had to be accelerated by ultrasound. Even with an excess of sodium hydride, no disodium salt could be detected. 3Na was found to be readily soluble in polar donor solvents like THF, Et<sub>2</sub>O, or glymes and insoluble in hexane, thus providing a convenient method to remove organic and inorganic impurities.

We have also used potassium hydride powder as a deprotonating agent. The reaction proceeded at 0 °C without ultrasound, and the evolution of hydrogen was finished after 1 h, leaving behind a white precipitate. Since this product was insoluble in ethers, we did not investigate it further. Comparison with the solubility of **3a/b**Na and **3a/b**Li and the dilithium salt **4Li<sub>2</sub>**, described below suggests, however, that the di- rather than the monopotassium derivative had formed.

A quasi-homogeneous deprotonation was achieved with *n*-BuLi. One equivalent of the reagent exclusively gave the monolithium salt **3a/b**Li whereas an excess gave the dilithium salt **4Li<sub>2</sub>**. The stepwise reaction could be followed conveniently when a suspension rather than a solution of **2a** (and **2b**) in THF was used at low temperature. The solid **2a** disappeared only after 1 equiv of *n*-BuLi had been added, and no further change was visible on addition of an excess. When the temperature of the solution was raised to -15 °C, the second deprotonation started and the dilithium salt precipitated.

3Na proved to be slightly more soluble than 3Li whereas **4Li<sub>2</sub>** was insoluble in THF, 1,4-dioxane, chelating ethers, DMSO, Et<sub>3</sub>N, and pure TMEDA. Interestingly, **4Li<sub>2</sub>** could be dissolved in a mixture of THF/TMEDA with a distinct optimum for a TMEDA content of 10–20% at 25 °C. This may be interpreted as the cleavage of a coordination polymer giving **4Li<sub>2</sub>(TMEDA)<sub>2</sub>**, which dissolves in THF. Similarly, cleavage was effected by the addition of an excess of CpNa in THF, which points to the formation of a sextuple ion comparable to the triple ion derived from CpLi.<sup>16</sup> **4Li<sub>2</sub>** could be also dissolved in hexamethylphosphoric triamide (HMPT) giving a deep purple solution, which did not show <sup>13</sup>C NMR signals of THF. This is further evidence for the formation of a solvent-free co-

(9) Shologon, I. M.; Romantsevich, M. K. *J. Org. Chem. USSR (Engl. Transl.)* 1966, 36, 1836.

(10) Schaaf, R. L.; Kan, P. T.; Lenk, K. T.; Deck, E. P. *J. Org. Chem.* 1960, 25, 1986.

(11) Hiermeier, J. Dissertation, Technische Universität München, 1989.

(12) Grishin, Yu. K.; Sergeev, N. M. Ustyynyuk, Yu. A. *Org. Magn. Reson.* 1987, 4, 377.

(13) Blümel, J.; Köhler, F. H. *J. Organomet. Chem.* 1988, 340, 303.

(14) Belsky, V. K.; Zemlyansky, N. N.; Borisova, I. V.; Kolosova, N. D.; Beletskaya, I. P. *Cryt. Struct. Commun.* 1982, 11, 497.

(15) Cooper, M. A.; Elleman, D. D.; Pearce, C. D.; Manatt, S. L. *J. Chem. Phys.* 1970, 53, 2343.

(16) Paquette, L. A.; Bauer, W.; Sivik, M. R.; Bühl, M.; Schleyer, P. v. R. *J. Am. Chem. Soc.* 1990, 112, 8776.

Table II.  $^{29}\text{Si}$  NMR Shifts<sup>a</sup> of 2a/b, 3a/bLi, 3a/bNa, and 4Li<sub>2</sub>

compd	solvent	position of nuclei <sup>b</sup>	
		4	8
2a	C <sub>6</sub> D <sub>6</sub>	-7.82	-7.82
2a	THF	-8.16	-8.16
2b	C <sub>6</sub> D <sub>6</sub>	4.81	-19.28
2b	THF	4.61	-19.71
3a/bLi	THF <sup>c</sup>	-7.85	-23.73
3a/bNa	THF <sup>d</sup>	-7.84	-23.61
4Li <sub>2</sub>	THF <sup>e</sup>	-28.76	-28.76

<sup>a</sup>  $\delta$  values at room temperature relative to internal (Me<sub>3</sub>Si)<sub>2</sub>O with  $\delta(^{29}\text{Si})$  6.87. <sup>b</sup> Numbering shown in Schemes I and II. <sup>c</sup> At -17 °C. <sup>d</sup> At -14 °C. <sup>e</sup> In the presence of CpNa.

ordination polymer 4Li<sub>2</sub> in step d of Scheme II.

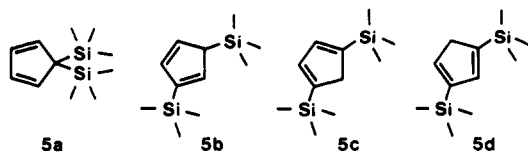
**Characterization of the Anions by NMR Spectroscopy.** Simple <sup>13</sup>C and <sup>1</sup>H NMR spectra with only four and three resonances, respectively, were obtained for the dianion 4, which is in accord with D<sub>2h</sub> symmetry. Inspection of the data in Table I shows that for the five-membered ring the <sup>1</sup>J(CH) values are rather small in HMPT and that the <sup>13</sup>C NMR signals are shifted more to low frequency when THF/TMEDA is used as solvent. This reflects the formation of solvent-separated ion pairs in the first and of contact ion pairs in the latter solvent.<sup>17</sup>

The <sup>29</sup>Si NMR spectra are simple and thus advantageous for the investigation of mixtures of the anions and/or the precursors 2a/b. The chemical shifts given in Table II reflect the bonding situation of the silicon atom (vinylic, allylic, or next to Cp anion), which in turn leads to a straightforward signal assignment.

The NMR spectra of the monoalkali-metal derivatives 3Li and 3Na were found to be temperature dependent. As an example, a series of <sup>13</sup>C NMR spectra of 3Na are shown in Figure 1. At -10 °C each of the 14 carbon atoms gives a separate signal in accord with C<sub>s</sub> symmetry (see Scheme II). The spectrum is composed of a Cp<sup>-</sup> part (110–120 ppm), a Me<sub>2</sub>Si part, and the resonances of the cyclopentadiene part. The assignment is therefore similar to that of 2a/b. C1 and C3 are distinguished independently by the fact that the resonances of C2 and C3 form a coalescence pair (see below), and C6 is distinguished from C5 and C7 because it is not engaged in coalescence.

On raising of the temperature, the signals broaden and, depending on the shift differences of the coalescing resonances, high-temperature-limiting spectra are seen; about 60 and 100 °C temperatures are necessary for the anionic and Me<sub>2</sub>Si parts, respectively. At 140 °C only the (averaged) signals of C2/3 and C8a appear whereas that of C1/3a (expected around 100 ppm) is still buried in the noise.

The analysis shows 3 to be an unusual case in the well-established<sup>18</sup> world of fluxional main-group derivatives of Cp. The most simple analogue of 3 is 5,5-bis(trimethylsilyl)cyclopentadiene (5), which has been studied in detail by Ustynyuk et al.<sup>19</sup> At -30 °C 5 has been shown to exist as a mixture of the isomers 5a/d, among which 5a



(17) Ogorodnikova, N. A.; Koridze, A. A.; Fedin, E. I.; Petrovskii, P. V. *Bull. Acad. Sci. USSR, Div. Chem. Sci. (Engl. Transl.)* 1983, 1847.

(18) Jutzi, P. *Chem. Rev.* 1986, 86, 983.

(19) Ustynyuk, Yu. A.; Kisin, A. V.; Pribytkova, I. M.; Zenkin, A. A.; Antonova, N. D. *J. Organomet. Chem.* 1972, 42, 47.

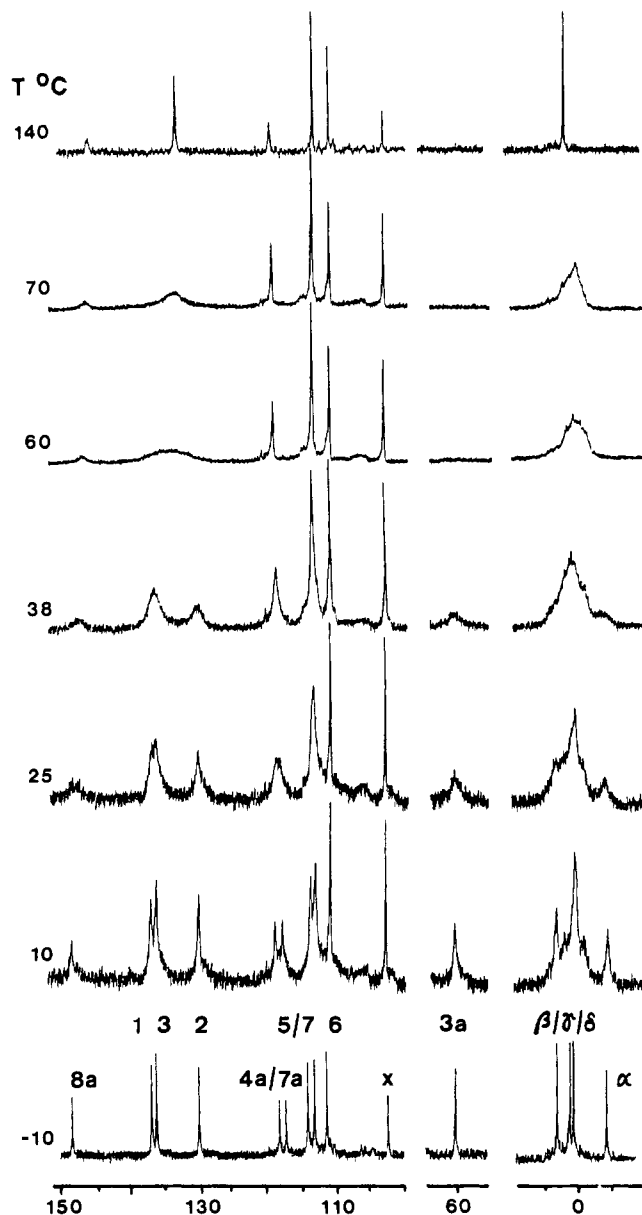
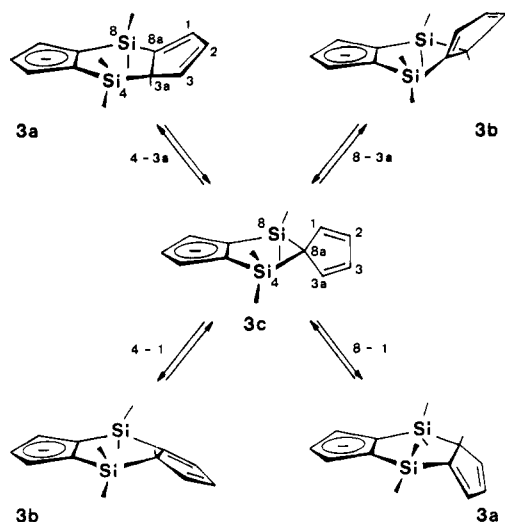


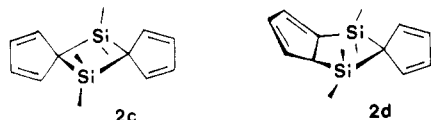
Figure 1. Temperature dependence of the <sup>13</sup>C{<sup>1</sup>H} NMR spectra of 3a/bNa dissolved in THF or triglyme (140 °C) (scale in ppm; × = impurity (Cp<sup>-</sup>)).

is by far the most stable (94%), and no isomers with vicinal silyl groups have been detected. By contrast, vicinal substitution was expected for the monoanion 3 on the basis of the known structure of the precursors 2a/b. We could confirm this by the NMR spectra, which showed no other isomer below 0 °C. There is now general agreement that the dynamic behavior of silylated Cp's is caused by 1,2-metallotropic rearrangements and that proton shifts occur only at high temperature.<sup>18</sup> When this is applied to 5, the interconversion of the isomers must be ascribed to both degenerate and nondegenerate 1,2-shifts, although Ustynyuk et al.<sup>19</sup> claimed 1,3-shifts to proceed as well. Apart from symmetry-control arguments, one of the conceivable 1,3-shifts may be excluded for 3 because it would lead to an unstable [4.2.1]bicyclic structure with a bridgehead double bond. For the same reason two successive 1,2-shifts leading to a 1,3-disilylated Cp and beyond this a merry-go-round silyl shift may be ruled out. Thus, we are left with the simple scheme shown in Figure 2. At low temperature the two stable enantiomers 3a/b are seen. Obviously, a metallotropic rearrangement can only occur via the isomer 3c, which may be regarded as a 1,3-disila-



**Figure 2.** Silatropic rearrangements of **3a/b**. The numbering of **3c** reflects the identity of the carbon atoms after silatropic shift starting from the numbered enantiomer **3a**.

cyclopent-4-ene derivative. The fact that **3c** is not observed by a separate set of NMR signals below 0 °C points to a high-energy species that is perceptibly populated only at high temperature where average signals are seen. The resonance of C8a should be most suitable to prove the equilibrium  $3a/b \rightleftharpoons 3c$  because it changes from olefinic to aliphatic and vice versa whereas C2/3 remain olefinic and C1/3a are heavily broadened. It can be seen in Figure 1 that the signal of C8a moves to low frequency on increasing the temperature, as expected for an increasing concentration of **3c**. This substantiates previous suggestions,<sup>6-7</sup> according to which **2c/d** should be intermediates



during the formation of **2a/b** (step b in Scheme I). On the basis of the present work, however, **2d** (and its enantiomer) must be considered as energetically more favorable intermediates.

In **3c** both Si4 and Si8 may form a new bond with C1 or C3a; this is indicated by the numbers assigned to the arrows in Figure 2. Consequently, there are two different ways of performing two successive 1,2-shifts starting from **3a** (or **3b**): (i) Only one atom (C or Si) is changed in the new bond. This leads to the second enantiomer, and the rearrangement is nondegenerate. Note that rapid exchange of this type can average the NMR signals only in the Cp<sup>-</sup> part (giving a 2/2/1 pattern) and the silyl groups (giving a 2/2 pattern) whereas all carbon atoms of the cyclopentadiene part retain their identity and give five signals. Since this is not observed, the following must (also) proceed. (ii) Both atoms are changed in the new bond, the same isomer is formed (degenerate rearrangement), and the signal averaging corresponds to the experimental results. In the latter process only C6 and C8a should be unaffected and yet a signal broadening was observed for C8a (Figure 1). This must be due to a "hidden partner exchange"<sup>20</sup> with **3c** being the hidden partner. From the maximum half-width  $\Delta^{\max} \approx 150$  Hz observed at 29 °C, and a shift difference  $\Delta\nu \approx 6200$  Hz for C8a in **3a/c**,<sup>21</sup> a frac-

pair of nuclei	field, T	temp, <sup>a</sup> K	$\Delta\nu$ , <sup>b</sup> Hz	$k_c$ , <sup>c</sup> s <sup>-1</sup>
C2/3	6.34	331.0	416.2	924.6
C2/3	4.70	325.0	308.2	684.6
C5/7	6.34	299.3	62.9	139.7
C5/7	4.70	294.2	47.8	106.2
C4a/7a	6.34	300.3	65.9	146.4
C4a/7a	4.70	293.5	46.4	103.1

<sup>a</sup> ± 1.5 K. <sup>b</sup> Shift difference ± 1.5 Hz. <sup>c</sup>  $k_c = (1/\sqrt{2})\pi\Delta\nu$ .

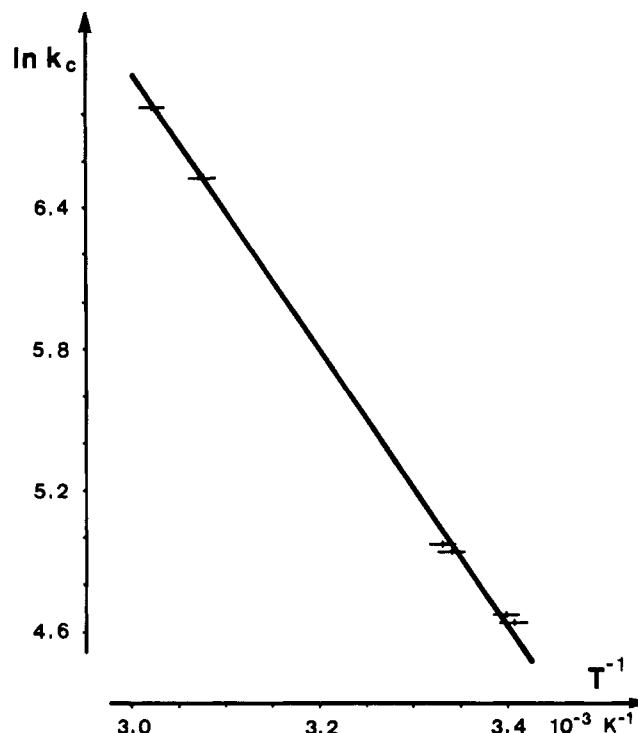
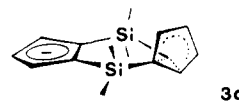


**Figure 3.** Arrhenius plot for the coalescence of selected <sup>13</sup>C NMR signals of **3a/bLi**.

tional population  $p = 0.024$  is estimated for **3c** at 29 °C by using the expression  $p = \Delta^{\max}/\Delta\nu$ .<sup>20a</sup>

For the corresponding enantiomeric lithium derivatives **3a/bLi** the <sup>13</sup>C NMR data were found to be very similar in the range -81 to 160 °C (Table III, supplementary material). This is in accord with  $\Delta\delta(^{13}\text{C})$  0.2 for CpLi and CpNa.<sup>17,22</sup> We have therefore restricted the evaluation of the activation barrier to **3a/bLi**. The coalescence temperature of three pairs of signals at two field strengths were determined and the rate constants  $k_c$  were calculated from the shift differences  $\Delta\nu$  (Table IV). These data gave the Arrhenius plot shown in Figure 3, from which an activation energy  $E_a = 48.5 \pm 2.3$  kJ mol<sup>-1</sup> (linear regression analysis  $48.2 \pm 1.3$  kJ mol<sup>-1</sup>) was obtained for two successive 1,2-shifts. This is about 12 kJ mol<sup>-1</sup> bigger than found for a single 1,2-shift in **5a**.<sup>19</sup> We ascribe the increase of the barrier to the effect of ring strain, which is less important for the ground state than for the transition state **3d**. A



model shows that the central part is intermediate between

(21)  $\delta(^{13}\text{C}5)$  57.0 of the very similar compound **5a** has been taken from: Grishin, Yu. K.; Luzikov, Yu. N.; Ustynuk, Yu. A. *Dokl. Chem. (Engl. Transl.)* 1974, 216, 315.

(22) Fischer, P.; Stadelhofer, J.; Weidlein, J. J. *Organomet. Chem.* 1976, 116, 65.

(20) (a) Anet, F. A. L.; Basus, V. J. *J. Magn. Reson.* 1978, 32, 339. (b) Okzawa, N.; Sorensen, T. S. *Can. J. Chem.* 1978, 56, 2737.

Table V. Selected Distances (Å)<sup>a</sup> and Angles (deg)<sup>a</sup> for 4Li<sub>2</sub>(TMEDA)<sub>2</sub>

Li-Cp1	2.357 (3)	Si-C11	1.882 (2)
Li-Cp2	2.297 (3)	Si-C12	1.883 (2)
Li-Cp3	2.247 (3)	Si-Cp1	1.848 (2)
Li-Cp4	2.283 (3)	Si-Cp5*	1.847 (2)
Li-Cp5	2.351 (3)	Cp1-Cp2	1.424 (2)
Li-N1	2.150 (3)	Cp2-Cp3	1.408 (3)
Li-N2	2.255 (3)	Cp3-Cp4	1.406 (2)
Li-D <sup>b</sup>	1.97	Cp4-Cp5	1.418 (2)
D-D*	4.96	Cp5-Cp1	1.448 (2)
Cp1-Si-C11	109.6 (1)	Cp5-Cp1-Si	124.5 (1)
Cp1-Si-C12	113.4 (1)	Cp1-Cp5-Si*	126.5 (1)
Cp1-Si-Cp5*	108.9 (1)	Cp1-Cp2-Cp3	108.8 (2)
C11-Si-Cp5*	112.9 (1)	Cp2-Cp3-Cp4	108.0 (1)
C12-Si-Cp5*	108.5 (1)	Cp3-Cp4-Cp5	109.3 (2)
C11-Si-C12	104.1 (1)	Cp4-Cp5-Cp1	106.8 (1)
N1-Li-N2	82.5 (1)	Cp5-Cp1-Cp2	107.2 (1)

<sup>a</sup>Esd's in units of the last significant figure in parentheses.

<sup>b</sup>Centroid of the Cp ring. \*Starred and unstarred atoms are interrelated by an inversion center.

the favorable six-membered ring of **3a/b** and the five-membered ring of the high-energy isomer **3c**. Similar to 4Li<sub>2</sub>, the alkali-metal derivatives of **3a/b** should be present as contact ion pairs in most solvents and they should therefore exist as diastereomers. However, only one set of <sup>13</sup>C NMR signals was observed down to -81 °C, which means that the metal exchange is fast under our conditions.

**Solid-State Structure of 4Li<sub>2</sub>.** The dilithium salt of the dianion **4** could be crystallized in the presence of TMEDA, and the X-ray structure analysis showed that 4Li<sub>2</sub>(TMEDA)<sub>2</sub> had formed. Its structure (Figure 4 and Table V) consists of two dimethylsilyl-bridged Cp anions, each of which is capped by a Li(TMEDA) moiety at opposite faces. The latter moieties are puckered. Their orientation conforms to the overall crystallographic symmetry C<sub>i</sub> of the whole molecule (space group P $\bar{1}$ , Z = 1). The anti arrangement is expected from the electrostatic interaction of the charges;<sup>23</sup> it has been found experimentally for the lithium derivatives of the dianions of naphthalene,<sup>24</sup> anthracene,<sup>25</sup> and pentalene,<sup>26</sup> and it has been shown to be energetically preferred in many di-lithiated polynuclear aromatics by MNDO calculations.<sup>26-28</sup>

As 4Li<sub>2</sub>(TMEDA)<sub>2</sub> is one of the few crystallographically examined lithium cyclopentadienyls with almost ideal metallocene structure ( $\eta^5$  coordination of lithium to the cyclopentadienyl ring),<sup>26,31,32</sup> a comparison of some of the

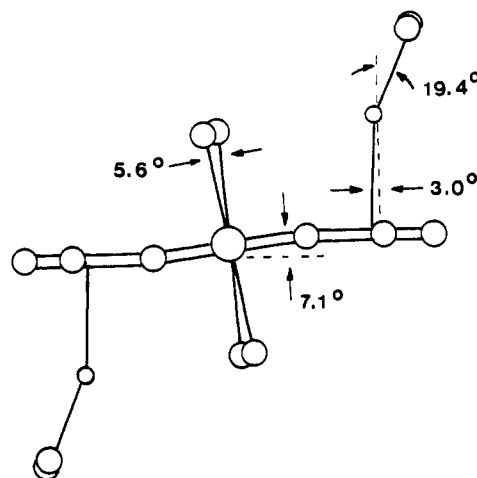
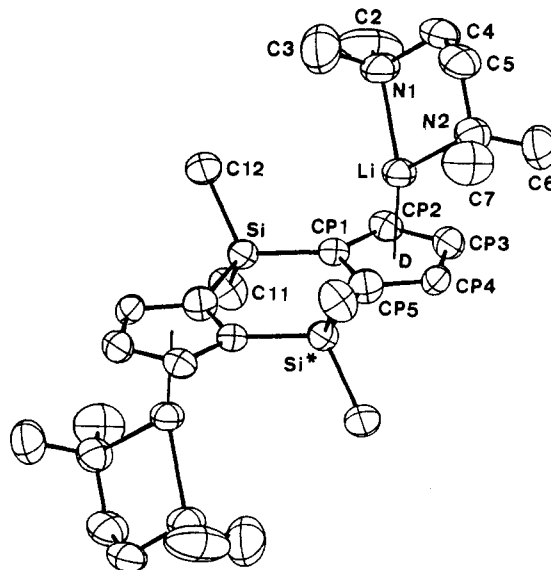


Figure 4. Top: ORTEP drawing of the molecular geometry of 4Li<sub>2</sub>(TMEDA)<sub>2</sub> (without hydrogen atoms) and atom numbering as used in Tables V and VII and Tables VIII and IX (supplementary material). Displacement ellipsoids are at the 50% probably level. Bottom: Side view with selected angles.

structural details of the metal coordination is of special interest. In 4Li<sub>2</sub>(TMEDA)<sub>2</sub> the Li-C(Cp) distances vary between 2.247 (3) and 2.357 (3) Å resulting in a Li-centroid(Cp) distance of 1.97 Å (Table V). Not surprisingly, the distance Li-Cp3 (most distant from the bridging silyl groups) is shortest, while Li-Cp1/5 is longest. This is certainly in large part due to steric interactions between the Me<sub>2</sub>Si bridges and the Li(TMEDA) fragment, which also account for other peculiarities in the molecular structure discussed further below. It is also observed in (Me<sub>3</sub>SiCp)Li(TMEDA)<sup>32</sup> whereas, in the series [(Me<sub>3</sub>Si)<sub>3</sub>Cp]Li(B) (B = TMEDA, quinuclidine, PMDETA, THF),<sup>31</sup> the evidence is less clear-cut due to the multiple silyl substitution of the Cp ring. Independent of these rather subtle differences, the overall Li-C(Cp) distances, as best evident in the Li-centroid(Cp) separations, seem to be markedly influenced by the donor molecules coordinated to lithium,<sup>31</sup> the monodentate quinuclidine allowing for the closest LiCp coordination. The Li-D (D = centroid of the Cp ring) distance of 1.97 Å observed in 4Li<sub>2</sub>(TMEDA)<sub>2</sub> directly compares to the values previously found in the other Li(TMEDA) species.<sup>31,32</sup>

As can be seen from the side view in Figure 4, the dianion has a flat skeleton in which the interplanar angle

(23) Streitwieser, A., Jr.; Swanson, J. T. *J. Am. Chem. Soc.* **1983**, *105*, 2502. Note that anti instead of trans is preferred in the present paper in order to facilitate the comparison with similar compounds<sup>3</sup> that adhere to the syn/anti terminology.

(24) Brooks, J. J.; Rhine, W.; Stucky, G. D. *J. Am. Chem. Soc.* **1972**, *94*, 7346.

(25) Rhine, W. E.; Davis, J.; Stucky, G. D. *J. Am. Chem. Soc.* **1975**, *97*, 2079.

(26) Stezowski, J. J.; Hoier, H.; Wilhelm, D.; Clark, T.; Schleyer, P. v. R. *J. Chem. Soc., Chem. Commun.* **1985**, 1263.

(27) Sygula, A.; Lipkowitz, K.; Rabideau, P. W. *J. Am. Chem. Soc.* **1987**, *109*, 6602.

(28) Bausch, J. W.; Gregory, P. S.; Olah, G. A.; Surya Prakash, G. K.; Schleyer, P. v. R.; Segal, G. A. *J. Am. Chem. Soc.* **1989**, *111*, 3633.

(29) (a) Alexandratos, S.; Streitwieser, A., Jr.; Schaefer, H. F., III. *J. Am. Chem. Soc.* **1976**, *98*, 7959. (b) Waterman, K. C.; Streitwieser, A., Jr. *J. Am. Chem. Soc.* **1984**, *106*, 3138.

(30) Rhine, W. E.; Stucky, G. D. *J. Am. Chem. Soc.* **1975**, *97*, 737.

(31) (a) Jutzi, P.; Schlüter, E.; Krüger, C.; Pohl, S. *Angew. Chem.* **1983**, *95*, 1015; *Angew. Chem., Int. Ed. Engl.* **1983**, *22*, 994. (b) Jutzi, P.; Schlüter, E.; Pohl, S.; Saak, W. *Chem. Ber.* **1985**, *118*, 1959. (c) Jutzi, P.; Leffers, W.; Pohl, S.; Saak, W. *Chem. Ber.* **1989**, *122*, 1449.

(32) Lappert, M. F.; Singh, A.; Engelhardt, L. M.; White, A. H. *J. Organomet. Chem.* **1984**, *262*, 271.

between the six-membered ring and both Cp planes is 172.9°. Owing to the crystallographic  $C_i$  symmetry the latter are parallel with a separation of 0.37 Å. The slight folding of the dianion leads to a bending of the Cp substituents away from the lithium. Such a bending has been predicted on the basis of ab initio calculations;<sup>29</sup> it varies between 0.2 and 6.8° depending on the basis set. On the other hand, X-ray work on (indenyl)Li(TMEDA),<sup>30</sup> [(Me<sub>3</sub>Si)<sub>3</sub>Cp]Li(B) (B = TMEDA, quinuclidine, PMDETA, THF),<sup>31</sup> and (Me<sub>3</sub>SiCp)Li(TMEDA)<sup>32</sup> has revealed no or very little bending except for B = THF.<sup>31c</sup> It is therefore likely that the interplanar angles in 4Li<sub>2</sub>(TMEDA)<sub>2</sub> are partly due to steric interactions between the Me<sub>2</sub>Si fragments and the Li(TMEDA) moieties. Such an interaction is also evident from the following facts: (i) The orientation of the vector N1–N2 relative to the longer axis of the dianion is almost perpendicular rather than close to parallel as found for other dianions.<sup>24–26</sup> (ii) The plane N1–Li–N2 is bent away from the MeSi groups. (iii) The planes C11–Si–C12 and C11\*–Si\*–C12\* include an angle of 5.6° such that the MeSi groups adapt themselves to the puckering of the Li(TMEDA) moieties. Note that the distances C3–C12 and C7–C11\* are only 3.94 and 3.76 Å, respectively. (iv) The vector Li–D (Figure 4) is bent away from the Me<sub>2</sub>Si fragments such that an angle of 3.0° is formed with the normal to the Cp plane.

The anti arrangement of Li(TMEDA) found for the solid state should be also preferred for the formation of contact ion pairs in solution, which in turn should yield anti derivatives after the reaction with suitable transition-metal compounds. On the other hand, steric congestion similar to that in 4Li<sub>2</sub>(TMEDA)<sub>2</sub> will reduce the stability of the contact ion pairs so that transition-metal derivatives of 4 with both syn and anti arrangements should be accessible. This is currently being examined in our laboratory.

### Experimental Section

All reactions and physical measurements were carried out under exclusion of air by using the standard Schlenk equipment, NMR tubes with ground-glass joints and stoppers, and oxygen-free solvents, which were purified by standard methods. All glassware was flame-dried in vacuo. The NMR spectra were obtained with Bruker CXP 200 and Jeol JNM GX 270 spectrometers. If not stated otherwise, the signals of the deuterated solvents were used as an internal reference; conversion relative to TMS was done by using  $\delta(^1\text{H}/^{13}\text{C})$  7.15/128.0 for benzene,  $\delta(^{13}\text{C})$  25.2/67.4 for THF-*d*<sub>6</sub>,  $\delta(^{13}\text{C})$  25.8/67.9 for THF,  $\delta(^{13}\text{C})$  36.5 for HMPT,  $\delta(^{13}\text{C})$  72.2/70.7/58.8 for triglyme, and  $\delta(^{13}\text{C})$  141.4/127.2/128.7/126.1 and  $\delta(^1\text{H})$  7.40/7.16/7.08 for biphenyl-*d*<sub>10</sub>.

**Cyclopentadienyldimethylchlorosilane (1).** From a freshly prepared solution of CpNa in THF (1000 mL, 2.02 M) the solvent was removed under reduced pressure. The remainder was suspended in 700 mL of diethyl ether and cooled to –20 °C, and a precooled mixture (–20 °C) of 542 g (4.2 mol) of dimethylchlorosilane and 300 mL of diethyl ether was added quickly under vigorous stirring. After being stirred another 30 min at –20 °C the mixture was brought to ambient temperature and the suspension was allowed to settle. The liquid was filtered over Na<sub>2</sub>SO<sub>4</sub>, the solvent and unreacted Me<sub>2</sub>SiCl<sub>2</sub> were removed at 0 °C/40 mbar, and after distillation of the remainder (20-cm Vigreux column, 25 °C/1.3 × 10<sup>–5</sup> bar) 249 g (77.7% relative to CpNa) of 1 was obtained as a colorless liquid.

**4,4,8,8-Tetramethyltetrahydro-4,8-disila-s-indacenes 2a/b.** A 150-mL (0.95-mol) amount of 1 diluted by 500 mL of pentane was cooled to –78 °C, and 559 mL of a 1.7 M solution of *n*-butyllithium in hexane (0.95 mol) was added dropwise within 6 h. First the solution became cloudy, and then a white precipitate formed. The mixture was allowed to warm to room temperature, stirred for 1 week, and filtered over Na<sub>2</sub>SO<sub>4</sub>, and the solid was washed twice with 100 mL of pentane. From the combined solutions the solvents were stripped until about 600 mL was left. Gradual cooling to –20 °C afforded 44.0 g of a colorless crystalline

Table VI. Crystal Structure Data for 4Li<sub>2</sub>(TMEDA)<sub>2</sub>

formula	C <sub>26</sub> H <sub>50</sub> Li <sub>2</sub> N <sub>4</sub> Si <sub>2</sub>
$M_r$	488.77
cryst system	triclinic
space group	$P\bar{1}$ (No. 2)
<i>a</i> , Å	8.216 (1)
<i>b</i> , Å	9.014 (1)
<i>c</i> , Å	11.527 (1)
$\alpha$ , deg	111.10 (1)
$\beta$ , deg	100.66 (1)
$\gamma$ , deg	88.85 (1)
<i>V</i> , Å <sup>3</sup>	781.69
<i>Z</i>	1
$d_{\text{calcd}}$ , g/cm <sup>3</sup>	1.038
$\mu(\text{Mo K}\alpha)$ , cm <sup>–1</sup>	1.3
<i>F</i> (000), e	268
<i>T</i> , °C	22
diffractometer	Enraf-Nonius CAD4
radiation ( $\lambda$ , Å)	Mo K $\alpha$ (0.710 69)
monochromator	graphite
scan	$\theta/2\theta$
scan width (in $\omega$ )	0.85 + 0.35 tan $\theta$
scan speed, deg/min	1–10
$((\sin \theta)/\lambda)_{\text{max}}$ , Å <sup>–1</sup>	0.594
<i>hkl</i> range	+11, ±12, ±16
standard reflcns	3, –1, –3; –2, –4, 0; 0, 3, –6
no. of reflcns (meas/unique)	2964/2737
<i>R</i> <sub>int</sub>	0.014
no. of reflcns obsd [ $F_o \geq 4.0\sigma(F_o)$ ]	2193
structure solution	direct methods (MULTAN-82)
H atoms (found/calcd)	19/6
no. of params refined	154
<i>R</i> <sup>a</sup>	0.051
<i>R</i> <sub>w</sub> <sup>b</sup>	0.075
(shift/error) <sub>max</sub>	0.65
$\Delta\rho_{\text{fin}}(\text{max})$ , e/Å <sup>3</sup>	0.23 at Cp4

$$^a R = \sum(|F_o| - |F_c|) / \sum|F_o|. \quad ^b R_w = [\sum w(|F_o| - |F_c|)^2 / \sum w F_o^2]^{1/2}; w = 1/\sigma^2(F_o).$$

material, which showed the <sup>1</sup>H NMR signals of 2a and 2b in a ratio of 2.4 (±0.1)/1 at 27 °C when dissolved in C<sub>6</sub>D<sub>6</sub>. Upon further concentration and cooling of the mother liquor another 9.0 g of crystals was obtained: total yield 45.7%; mp 107–8 °C. The product could be sublimed at 60 °C/10<sup>–5</sup> bar with essentially no loss of weight, yielding big crystals with mp 108–9 °C.

**2a:** <sup>1</sup>H NMR (C<sub>6</sub>D<sub>6</sub>, 294 K)  $\delta$  –0.40 (s, 6 H, H $\alpha/\gamma$ ), 0.41 (s, 6 H, H $\beta/\delta$ ), 3.46 (m, 2 H, H3a/7a), <sup>3</sup>*J*<sub>3a3</sub> ≈ <sup>4</sup>*J*<sub>3a1</sub> ≈ <sup>4</sup>*J*<sub>3a2</sub> = 1.0 Hz), 6.69 (m, 2 H, H2/6), <sup>3</sup>*J*<sub>23</sub> = 4.7 Hz, <sup>3</sup>*J*<sub>21</sub> = 2.0 Hz, <sup>4</sup>*J*<sub>23a</sub> = 0.8 Hz), 6.74 (m, 2 H, H3/7), <sup>3</sup>*J*<sub>32</sub> = 4.7 Hz, <sup>4</sup>*J*<sub>31</sub> = <sup>4</sup>*J*<sub>33a</sub> = 1.1 Hz), 6.97 (m, 2 H, H1/5), <sup>3</sup>*J*<sub>12</sub> = 2.0 Hz, <sup>4</sup>*J*<sub>13</sub> ≈ <sup>4</sup>*J*<sub>13a</sub> = 1.1 Hz); <sup>13</sup>C NMR (C<sub>6</sub>D<sub>6</sub>, 294 K)  $\delta$  –6.87 (C $\alpha/\gamma$ ), –2.87 (C $\beta/\delta$ ), 57.52 (C3a/7a), <sup>1</sup>*J*<sub>CH</sub> = 131.8 Hz), 131.25 (C2/6), <sup>1</sup>*J*<sub>CH</sub> = 162.4 Hz), 138.62 (C3/7), <sup>1</sup>*J*<sub>CH</sub> = 166.3 Hz), 139.92 (C1/5), <sup>1</sup>*J*<sub>CH</sub> = 163.3 Hz), 145.65 (C4a/8a); <sup>29</sup>Si NMR (C<sub>6</sub>D<sub>6</sub>, 294 K)  $\delta$  –7.82; <sup>29</sup>Si NMR (THF, 294 K)  $\delta$  –8.16.

**2b:** <sup>1</sup>H NMR (C<sub>6</sub>H<sub>6</sub>, 294 K)  $\delta$  –1.20 (s, 3 H, H $\beta$ ), –0.47/–0.36/0.25 (s and 3 H each, H $\gamma/\delta/\alpha$ ), 3.56 (m, 2 H, H3a/4a), <sup>3</sup>*J*<sub>3a3</sub> ≈ <sup>4</sup>*J*<sub>3a1</sub> ≈ <sup>4</sup>*J*<sub>3a2</sub> = 1.0 Hz), 6.58 (m, 2 H, H2/6), <sup>3</sup>*J*<sub>23</sub> = 4.7 Hz, <sup>3</sup>*J*<sub>21</sub> = 2.0 Hz, <sup>4</sup>*J*<sub>23a</sub> = 1.0 Hz), 6.64 (m, 2 H, H3/5), <sup>3</sup>*J*<sub>32</sub> = 4.7 Hz, <sup>4</sup>*J*<sub>31</sub> = 1.1 Hz, <sup>4</sup>*J*<sub>33a</sub> = 1.0 Hz), 6.85 (m, 2 H, H1/7), <sup>3</sup>*J*<sub>12</sub> = 1.9 Hz, <sup>4</sup>*J*<sub>13</sub> = 1.1 Hz, <sup>4</sup>*J*<sub>13a</sub> = 1.0 Hz); <sup>13</sup>C NMR (C<sub>6</sub>D<sub>6</sub>, 294 K)  $\delta$  –15.28 (C $\beta$ ), –5.25/0.48/1.04 (C $\gamma/\delta/\alpha$ ), 55.69 (C3a/4a), <sup>1</sup>*J*<sub>CH</sub> = 130.0 Hz), 131.35 (C2/6), <sup>1</sup>*J*<sub>CH</sub> = 162.4 Hz), 137.14 (C3/5), <sup>1</sup>*J*<sub>CH</sub> = 166.8 Hz), 138.79 (C1/7), <sup>1</sup>*J*<sub>CH</sub> = 162.4 Hz), 147.89 (C7a/8a); <sup>29</sup>Si NMR (C<sub>6</sub>D<sub>6</sub>, 294 K)  $\delta$  –19.28 (Si8), 4.81 (Si4); <sup>29</sup>Si NMR (THF, 294 K)  $\delta$  –19.71 (Si8), 4.61 (Si4).

**Reaction of 2a/b with Sodium Hydride.** Sodium hydride (2.6 g, 10.8 mmol) and 2a (1.2 g, 4.9 mmol) were mixed together in 100 mL of THF, and the suspension was kept in an ultrasonic bath at 45 °C for 5 days. The resulting red solution was decanted from excess NaH, THF was removed in vacuo, and the remainder was washed with pentane, giving 1.3 g of a white powder that, according to <sup>13</sup>C NMR spectroscopy, contained the 4,4,8,8-tetramethyl-3a,4,7a,8-tetrahydro-4,8-disila-s-indacene-3a-yl anion. The synthesis implies that it was the sodium salt 3Na. <sup>13</sup>C NMR (THF, 243 K):  $\delta$  148.1, 136.8, 136.0, 130.0, 118.8/117.6, 114.1/113.3, 111.1, 60.2, 3.2/0.7/0.4, –4.2 (C8a, C1, C3, C2, C4a/C7a, C5/C7, C6, C3a, C $\beta$ /C $\gamma$ /C $\delta$ , C $\alpha$ ). <sup>13</sup>C NMR (triglyme, 413 K):  $\delta$  145.9,

**Table VII. Fractional Atomic Coordinates and Equivalent Isotropic Displacement Parameters for  $4\text{Li}_2(\text{TMEDA})_2$** 

atom	$x/a$	$y/b$	$z/c$	$B_{\text{eq}}, \text{\AA}^2$
Si	0.45545 (9)	0.15472 (7)	0.43643 (6)	2.89 (1)
N1	0.1006 (3)	0.3276 (3)	0.7391 (2)	4.60 (5)
N2	0.2165 (3)	0.1386 (3)	0.8932 (2)	4.21 (5)
Cp1	0.5021 (3)	0.1855 (2)	0.6069 (2)	2.70 (5)
Cp2	0.5316 (3)	0.3326 (3)	0.7116 (2)	3.25 (5)
Cp3	0.5850 (3)	0.3008 (3)	0.8233 (2)	3.50 (6)
Cp4	0.5922 (3)	0.1349 (3)	0.7896 (2)	3.26 (5)
Cp5	0.5407 (3)	0.0600 (2)	0.6567 (2)	2.71 (5)
C11	0.6081 (4)	0.2778 (3)	0.4011 (2)	4.74 (7)
C12	0.2476 (4)	0.2266 (3)	0.3849 (3)	4.71 (7)
C2	0.1207 (5)	0.4799 (4)	0.7258 (4)	9.0 (1)
C3	-0.0250 (5)	0.2284 (6)	0.6327 (4)	8.9 (1)
C4	0.0469 (4)	0.3530 (4)	0.8592 (3)	4.98 (7)
C5	0.0500 (4)	0.2022 (4)	0.8871 (3)	5.10 (7)
C6	0.3242 (5)	0.2253 (4)	1.0150 (3)	6.17 (9)
C7	0.2039 (5)	-0.0306 (4)	0.8758 (3)	6.88 (9)
Li	0.3229 (5)	0.1988 (5)	0.7478 (4)	3.47 (9)

$$^a B_{\text{eq}} = \frac{1}{3}[a^2\beta_{11} + b^2\beta_{22} + c^2\beta_{33} + ab(\cos \gamma)\beta_{12} + ac(\cos \beta)\beta_{13} + bc(\cos \alpha)\beta_{23}]$$

133.4, 120.0, 113.6, 111.2, 0.4 (C8a, C2/3, C4a/7a, C5/7, C6, C $\alpha$ / $\beta$ / $\gamma$ / $\delta$ ; C1 and C3a not observed).

**Reaction of 2a/b with *n*-Butyllithium.** A solution of 1.83 g (7.5 mmol) of 2a in 50 mL of THF was cooled to -78 °C. To the resulting white suspension was added under stirring 4.3 mL of a 1.73 M solution of *n*-BuLi in hexane (7.4 mmol), giving a colorless solution. After removal of the cooling bath, the solvents were stripped until a few mL were left. Addition of 50 mL of pentane gave a white precipitate, from which the solvents were removed with a pipet. Drying in vacuo gave 1.74 g of a white powder that did not melt below 250 °C. The  $^{13}\text{C}$  NMR spectrum was very similar to that of 3Na and thus showed that it was the lithium salt 3Li.  $^{13}\text{C}$  NMR (THF, 253 K):  $\delta$  148.5, 137.4, 136.7, 130.4, 119.0/118.1, 115.0/114.1, 112.3, 60.8, 2.8/1.3/0.3, -4.5 (C8a, C1, C3, C2, C4a/C7a, C5/C7, C6, C3a, C $\beta$ /C $\gamma$ /C $\delta$ , C $\alpha$ ).  $^{13}\text{C}$  NMR (triglyme, 433 K):  $\delta$  144.5, 133.8, 120.3, 114.4, 112.3, 0.4 (C8a, C2/3, C4a/7a, C5/7, C6, C $\alpha$ / $\beta$ / $\gamma$ / $\delta$ ; C1 and C3a not observed).

When the reaction was carried out with 8.7 mL of a 1.73 M solution of *n*-BuLi in hexane (15.0 mmol), again a colorless solution was obtained. On raising of the temperature, the solution became cloudy at -15 °C, and a voluminous suspension formed on further heating to room temperature. The solid was allowed to settle, the solvent was removed with a pipet, and the remainder washed several times with pentane and dried in vacuo. The resulting white powder (1.8 g) did not melt below 250 °C. When it was redissolved in HMPT, NMR spectroscopy showed the presence of the 4,4,8-tetramethyl-3a,4,7a,8-tetrahydro-4,8-disila-s-indacene-3a,7a-diyl dianion, indicating that the powder contained the dilithium salt 4Li $_2$ .

A 200-mg sample of the solid was suspended in 20 mL of a 4/1 mixture of THF and TMEDA. After the mixture was stirred for 5 h at ambient temperature, the solid had dissolved partly. The clear solution was decanted, transferred into a Schlenk tube, and slowly cooled to -15 °C. After several weeks a crystal had formed that proved suitable for X-ray structure analysis.

**Crystal Structure Analysis of  $4\text{Li}_2(\text{TMEDA})_2$ .** Crystal data and a summary of data pertinent to data collection and refinement are collected in Table VI. Exact cell dimensions were obtained by least-squares refinement on the Bragg angles of 25 selected reflections centered on the diffractometer. Reduced cell calculations did not reveal symmetry higher than triclinic. Three standard reflections, measured after every 50 reflections, showed a nonlinear intensity decay of 31.4%, which was corrected for. A correction for absorption was not considered necessary. Refinement was done with anisotropic displacement parameters. The hydrogen atom positions were included as fixed atom contributions.

Atomic form factors for neutral, isolated atoms were those of Cromer and Waber;<sup>33</sup> those for hydrogen were based on the bonded, spherical atom model of Stewart, Davidson, and Simpson.<sup>34</sup> Corrections for anomalous scattering were applied for all atoms except hydrogen.<sup>35</sup> The programs used included the SDP suite of programs<sup>36</sup> and ORTEP<sup>37</sup> (molecular drawings), as well as locally written routines.

Table VII contains the fractional atomic coordinates of the non-hydrogen atoms. See the paragraph at the end of this paper for supplementary material available.

**Acknowledgment.** We gratefully acknowledge the assistance of Dr. N. Hertkorn in the NMR work, of M. Fritz in checking some experimental procedures, and of J. Riede in the X-ray work. We are also grateful for support from the Fonds der Chemischen Industrie and Wacker Chemie GmbH.

**Supplementary Material Available:** A table of temperature-dependent  $^{13}\text{C}$  NMR signal shifts for 3a/bLi and 3a/bNa (Table III) and listings of atomic parameters (Table VIII) and general displacement parameters (Table IX) (4 pages); a table of observed and calculated structure factors (Table X) (14 pages). Ordering information is given on any current masthead page.

(33) Cromer, D. T.; Waber, J. T. *Acta Crystallogr.* 1965, 18, 104.

(34) Stewart, R. F.; Davidson, E. R.; Simpson, W. T. *J. Chem. Phys.* 1965, 42, 3175.

(35) *International Tables for X-ray Crystallography*; Kynoch Press: Birmingham, England, 1974; Vol. IV. (Present distributor: Kluwer Academic Publishers, Dordrecht, The Netherlands.)

(36) Frenz, B. A. In *Computing in Crystallography*; Schenk, H., Olthof-Hazelkamp, R., van Koningsveld, H., Bassi, G. C., Eds.; Delft University Press: Delft, The Netherlands, 1978.

(37) Johnson, C. K. ORTEP-II. Report ORNL-5138; Oak Ridge National Laboratory: Oak Ridge, TN, 1976.